



Supplement of

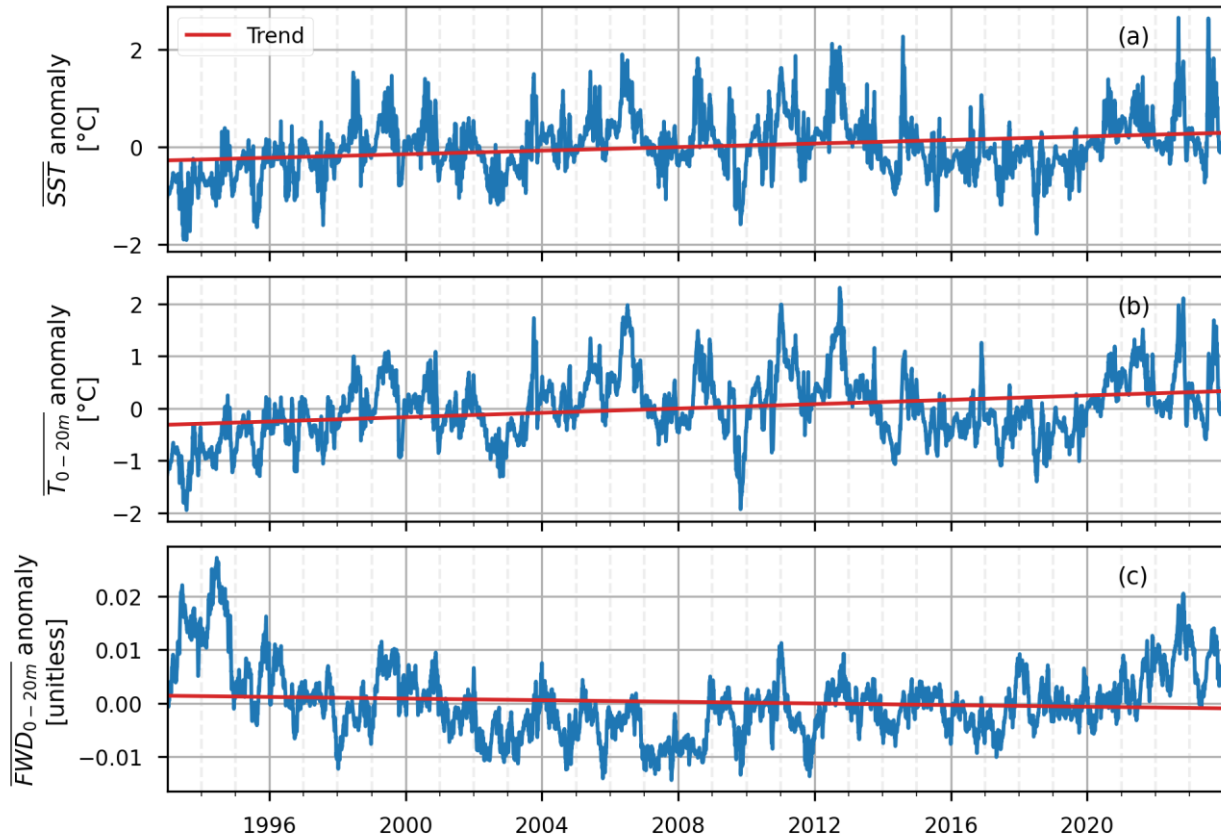
An analysis of the 2023 summer and fall marine heat waves on the Newfoundland and Labrador Shelf

Nancy Soontiens et al.

Correspondence to: Nancy Soontiens (nancy.soontiens@dfo-mpo.gc.ca)

The copyright of individual parts of the supplement might differ from the article licence.

1 **S1 Temperature and freshwater trends and sensitivity to climatological period**



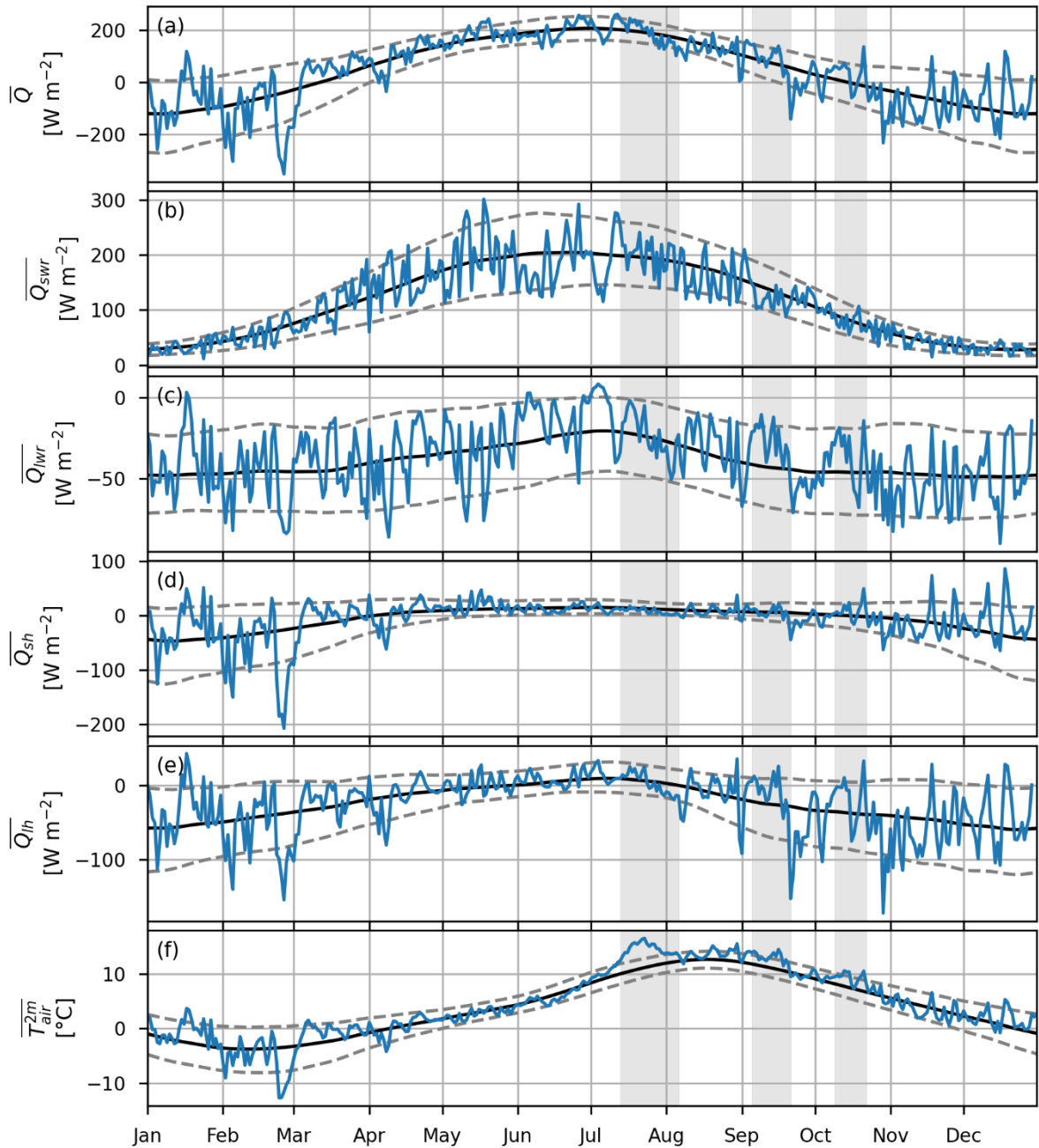
2

3 **Figure S1: Time series of the GLORYS12V1 (product ref. no. 1) (a) sea surface temperature anomaly, (b) 0 to 20 m vertically**
4 **averaged temperature anomaly, and (c) 0 to 20 m freshwater density anomaly over the NL Shelf. The trend for each time series is**
5 **computed using a linear regression.**

6

7 The selection of the climatological period is an important consideration when conducting a MHW study (Smith et al., 2025).
8 We explored the sensitivity of the MHW metrics to the climatological period by considering climatologies over 1993-2019
9 and 1996-2022. These two periods were selected to control for the relatively warm conditions from 2020-2022 and cold
10 conditions from 1993-1995 (Galbraith et al., 2024). We found that, relative to the 1993-2022 climatology, the duration of a
11 regional MHW event could be modified by up to four days. More typically, the duration was modified by a day or two. In
12 addition, the maximum intensity was no more than 0.19 °C different when compared to the original 1993-2022 climatological
13 period. The largest impact occurred during the October MHW over the entire NL Shelf which was shortened by seven days
14 when using the 1996-2022 period and lengthened by eight days when using the 1993-2019 period. Furthermore, when using
15 the 1993-2019 climatology, the temperature increase in late August shown in Fig. 4 (a) achieved the MHW definition on the

16 NL Shelf and the FC and GB regions both achieved MHWs in October. Finally, the two 5-day long MHWs in FC and NNS
17 were not long enough to meet the MHW definition when using the 1996-2022 climatology. Overall, our interpretations of the
18 factors contributing to MHWs were not impacted by modifying the climatological period.



20

21 **Figure S2: Time series of the ERA5 (product ref. no 2) (a) net surface heat flux, (b) net surface short-wave radiation, (c) net surface**
22 **long-wave radiation, (d) surface sensible heat flux, (e) surface latent heat flux, and (f) 2-metre air temperature. All fluxes are positive**
23 **downward, represent a daily average, and are spatially averaged over the NL Shelf region. Only grid cells entirely over ocean are**
24 **used in the spatial average. The 2023 time series is shown in blue, the 1993-2022 climatologies in black, and the 10th and 90th**
25 **percentiles in grey dashed. The NL Shelf MHW periods are represented by the grey shading.**

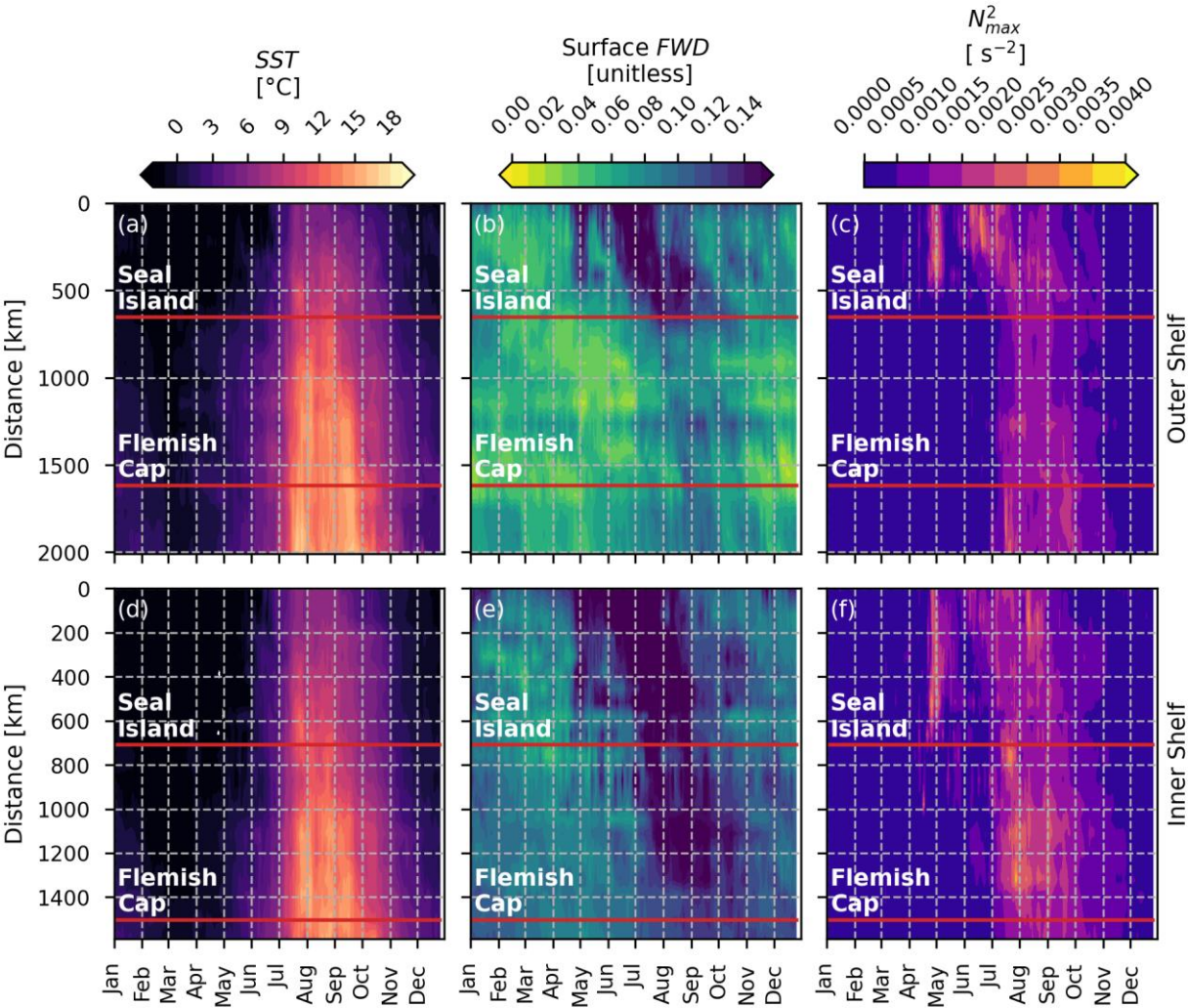


Figure S3: Time series of the GLORYS12V1 (product ref. no. 1) sea surface temperature (left), surface freshwater density (middle), and vertical maximum of the squared-buoyancy frequency (right) for year 2023 along the Outer Shelf (top) and Inner Shelf (bottom) transects (black dotted line in Fig. 1; 0 km here corresponding to the northern limit). The red lines represent the along-shelf locations of the Seal Island (upper) and Flemish Cap (lower) transects.

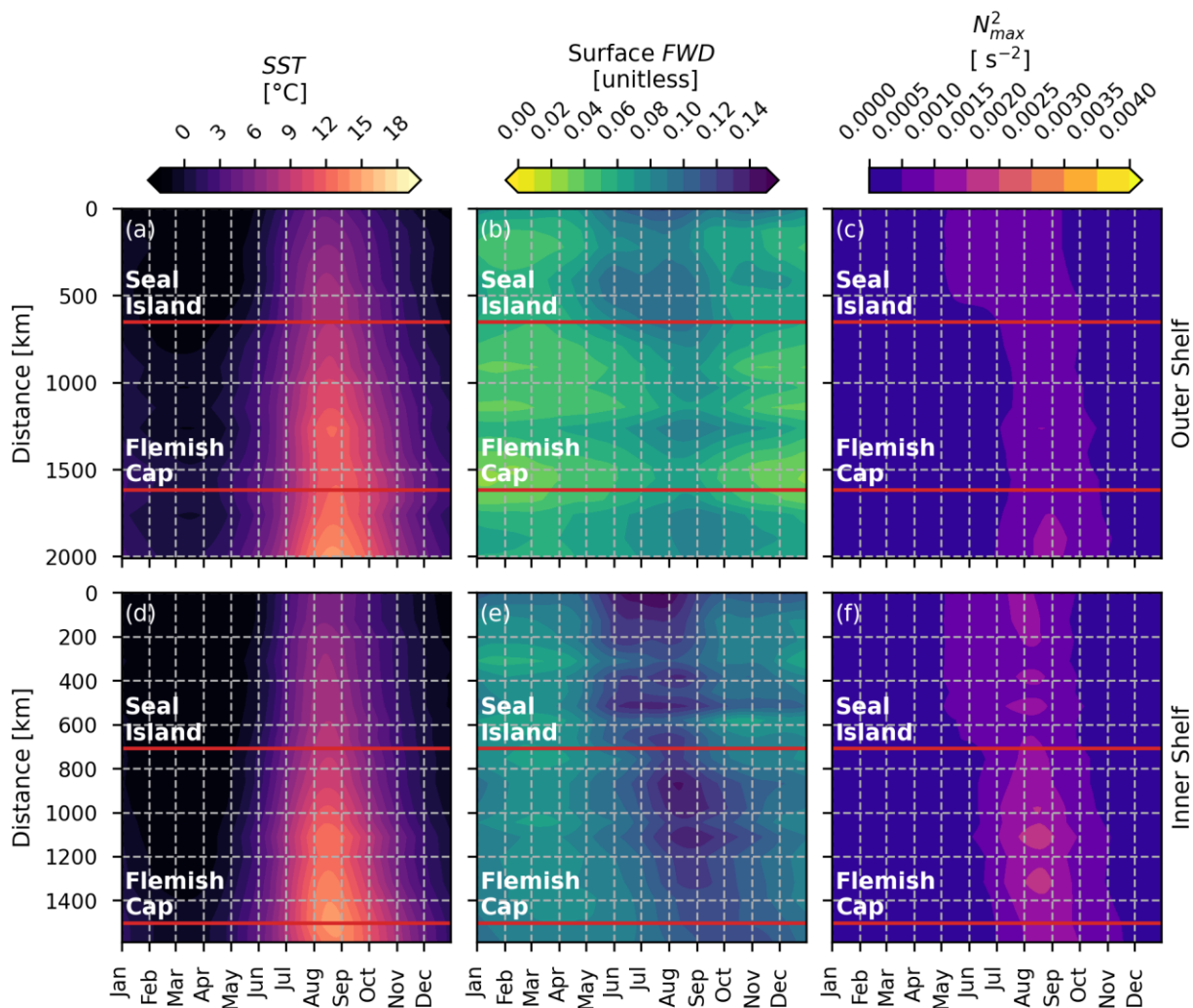
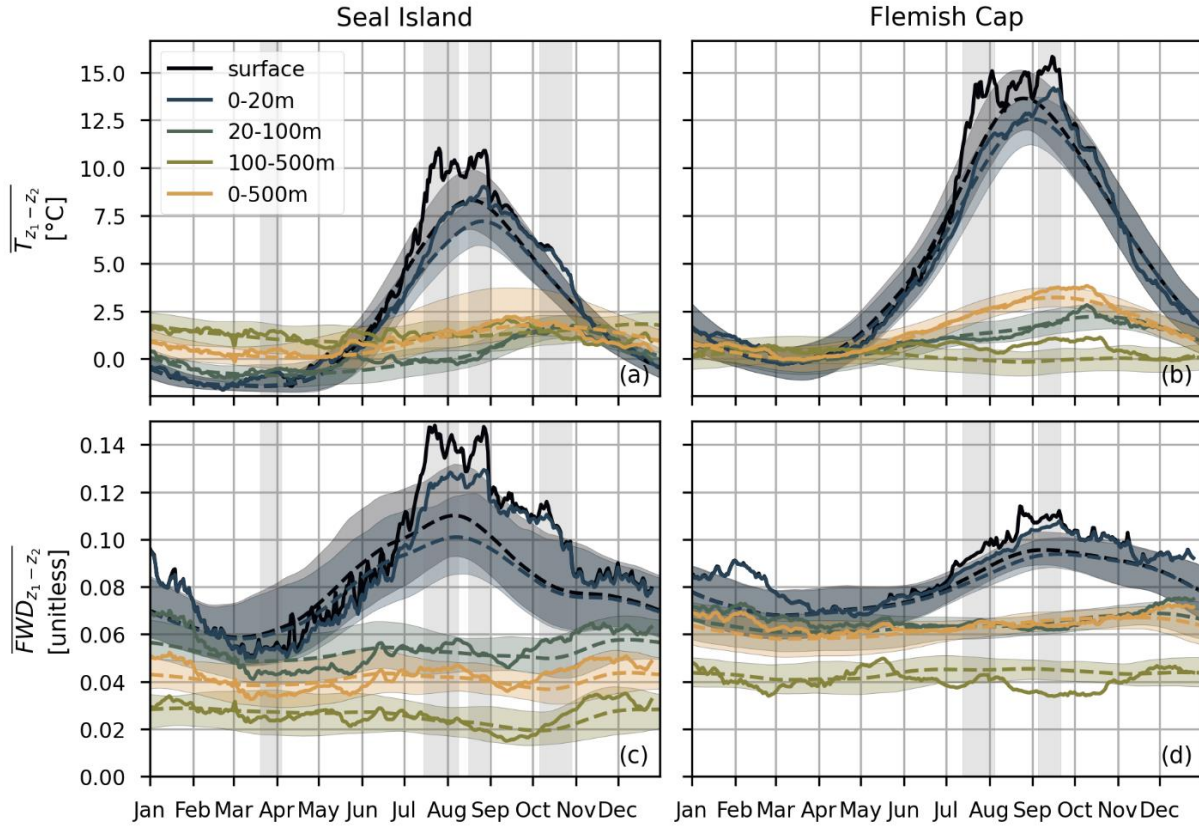


Figure S4: As in Figure S3 but for the 1993-2022 climatological fields.



35

36 **Figure S5: Depth-averaged temperature (top) and freshwater density (bottom) from GLORYS12V1 (product ref. no. 1) averaged**
 37 **across the Seal Island (left) and Flemish Cap transects (right). Results are shown out to the 500 m isobath for the surface (black), 0-**
 38 **20m (dark blue), 20-100m (dark green), 100-500m (light green), and 0-500m (orange). The solid line is the 2023 time series, the**
 39 **dashed line is the 1993-2022 climatology, and the shaded areas represent the 10th and 90th percentiles from the 1993-2022 period.**
 40 **Grey shaded rectangles represent heat wave periods based on SST along each transect. The scientific colour map batlow (Crameri**
 41 **2018) is used in this plot to prevent visual distortion of the data and exclusion of readers with colour-vision deficiencies (Crameri et**
 42 **al., 2020).**

43 **S5 Temperature and salinity contributions to stratification**

44 Temperature ($N_T^2(z)$) and salinity ($N_S^2(z)$) contributions to the stratification were approximated as follows (see e.g., Cyr et al.,
 45 2024):

$$N_T^2(z) \approx -g\alpha \frac{\partial T}{\partial z},$$

$$N_S^2(z) \approx g\beta \frac{\partial S}{\partial z},$$

48 where α and β are the coefficients of thermal expansion and haline contraction, respectively, g is the acceleration due to
 49 gravity, T and S are the conservative temperature and absolute salinity. We computed $N_T^2(z)$ and salinity $N_S^2(z)$ to determine

50 if changes in the squared-buoyancy frequency were driven by changes in temperature or salinity. Calculations for α , β , and g
 51 were carried out using the Python implementation of the Gibbs-Seawater (GSW) Oceanographic Toolbox (McDougall and
 52 Barker, 2011) at every grid cell in the GLORYS12V1 domain. The GLORYS12V1 (product ref. no. 1) temperature and salinity
 53 outputs were interpreted as conservative temperature and preformed salinity scaled by a factor of $u_{ps} = \frac{35.16504}{35} \text{g kg}^{-1}$ and
 54 absolute salinity was calculated using GSW. Vertical temperature and salinity gradients were calculated using a second-order
 55 central differences approximation, except at the upper and lower boundaries where a first-order approximation was employed.
 56 Then, $N_T^2(z)$ and $N_S^2(z)$ were evaluated at the depth where the squared-buoyancy frequency, $N^2(z)$, attains its maximum
 57 (N_{max}^2). Values are linearly interpolated to the Outer and Inner Shelf transects and compared with N_{max}^2 (Fig. S6 for 2023;
 58 Fig. S7 for 1993-2022 climatologies). Vertical salinity gradients were estimated to be the larger contributor to the stratification
 59 for the upstream portions of the transect (e.g., upstream of Seal Island, particularly for the Inner Shelf). For downstream regions
 60 in 2023, the vertical temperature gradients were the leading contributor to the stratification during the July MHW.

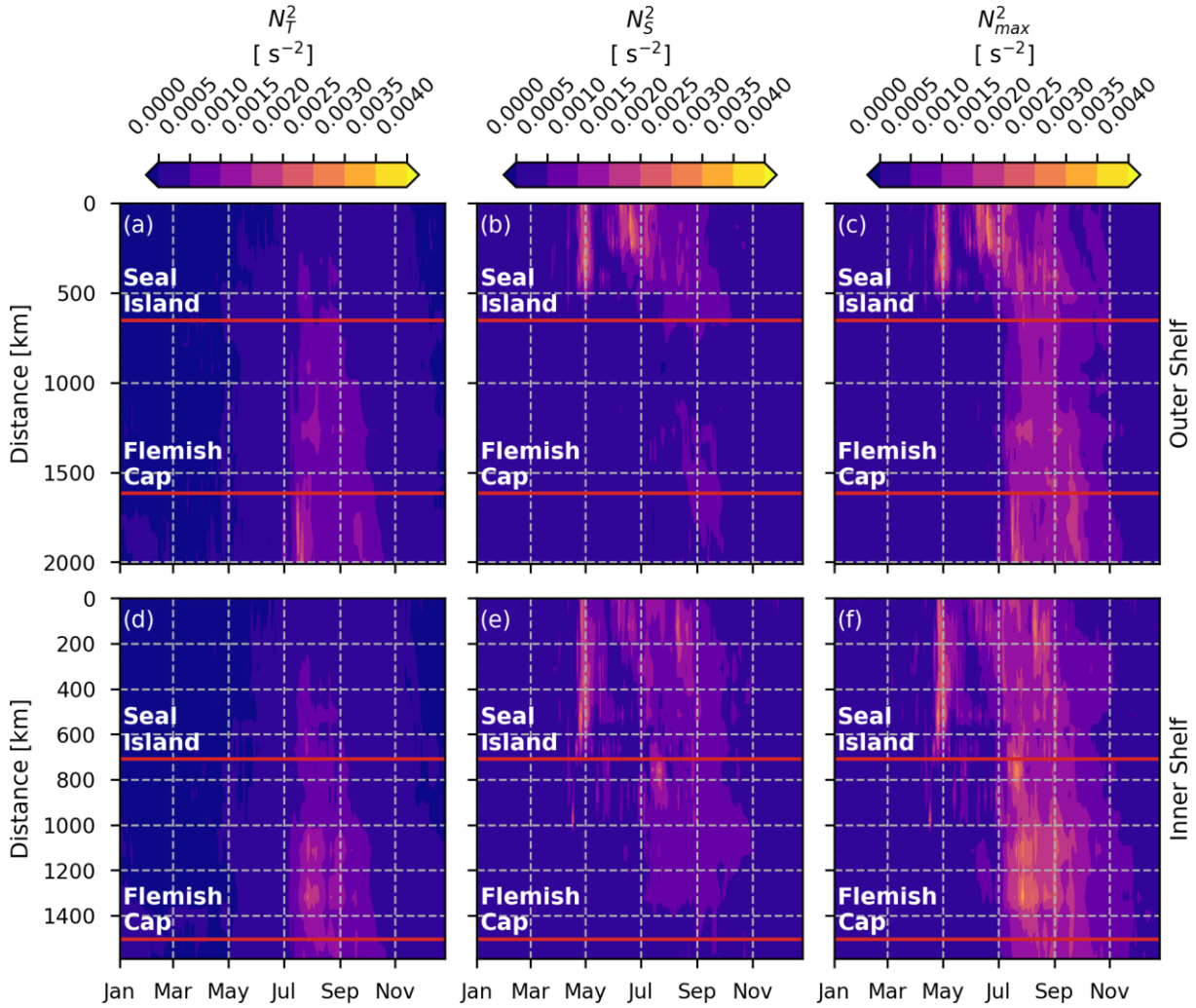


Figure S6: Time series of the temperature (N_T^2 ; left) and salinity (N_S^2 ; middle) contributions to the vertical of maximum squared-buoyancy frequency (N_{max}^2 ; right) for year 2023 along the Outer Shelf (top) and Inner Shelf (bottom) transects (black dotted line in Fig. 1; 0 km here corresponding to the northern limit). Values were estimated using the GLORYS12V1 (product ref. no. 1) temperature and salinity fields. The red lines represent the along-shelf locations of the Seal Island (upper) and Flemish Cap (lower) transects.

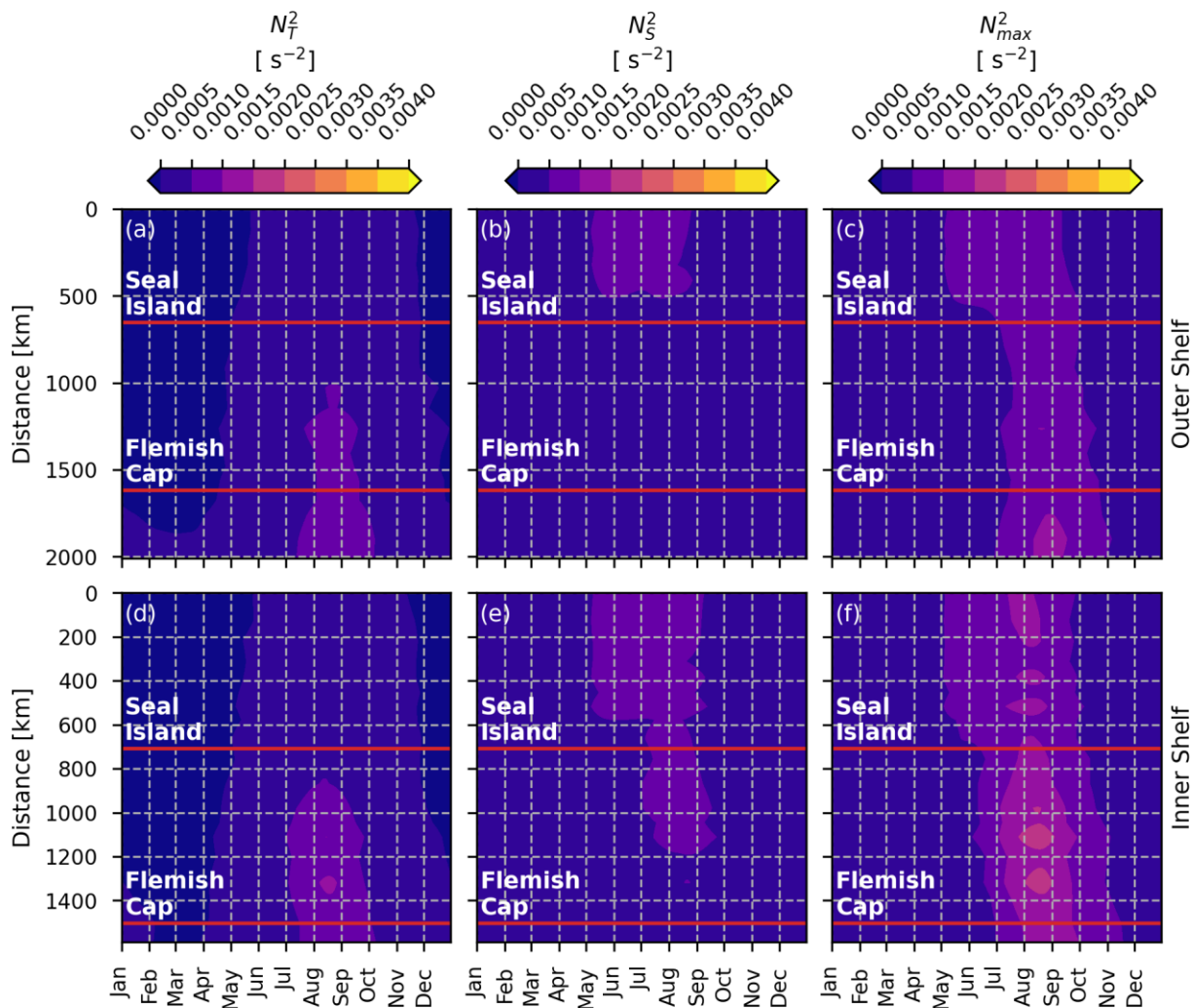


Figure S7: As in Fig. S6 but for the 1993-2022 climatological fields.

70 **References**

- 71 Crameri, F.: Scientific colour maps, Zenodo, doi:10.5281/ zenodo.1243862, 2018.
- 72
- 73 Crameri, F., Shephard, G. E. and Heron, P. J.: The misuse of colour in science communication, Nat. Commun., 11, 5444. doi:
- 74 10.1038/s41467-020-19160-7, 2020.
- 75
- 76 Cyr, F., Lewis, K., Bélanger, D., Regular, P., Clay, S., and Devred, E.: Physical controls and ecological implications of the
- 77 timing of the spring phytoplankton bloom on the Newfoundland and Labrador shelf, Limnol. Oceanogr. Lett.
- 78 <https://doi.org/10.1002/lol2.10347>, 2024.
- 79
- 80 Galbraith, P. S., Blais, M., Lizotte, M., Cyr, F., Bélanger, D., Casault, B., Clay, S., Layton, C., Starr, M., Chassé, J., Azetsu-
- 81 Scott, K., Coyne, J., Devred, E., Gabriel, C.-E., Johnson, C. L., Maillet, G., Pepin, P., Plourde, S., Ringuette, M. Shaw, J.-L.,
- 82 Oceanographic conditions in the Atlantic zone in 2023, Can. Tech. Rep. Hydro. and Ocean Sci., 379 : v + 39 p., 2024.
- 83
- 84 McDougall, T. J. and Barker, P. M.: Getting started with TEOS-10 and the Gibbs Seawater (GSW) Oceanographic Toolbox,
- 85 28 pp., SCOR/IAPSO WG127, ISBN 978-0-646-55621-5, 2011.
- 86
- 87 Smith, K. E., Sen Gupta, A., Amaya, D., A. Benthuisen, J. A., Burrows, M. T., Capotondi, A., Filbee-Dexter, K., Frölicher,
- 88 T. L., Hobday, A. J., Holbrook, N. H., Malan, N., Moore, P. J., Oliver, E. C. J., Richaud, B., Salcedo-Castro, J., Smale, D. A.,
- 89 Thomsen, M., and Wernberg, T.: Baseline matters: Challenges and implications of different marine heatwave baselines, Prog.
- 90 Oceanogr., 231, 103404, <https://doi.org/10.1016/j.pocean.2024.103404>, 2025.